JOURNAL OF SOLID STATE CHEMISTRY 94, 396–403 (1991)

The Eu Site Symmetry in $AEu(MoO_4)_2$ (A = Cs or Rb) Generating Saturated Red Luminescence

HAJIME YAMAMOTO,* SETSUKO SEKI,† AND TSUTOMU ISHIBA

Central Research Laboratory, Hitachi Ltd., P.O. Box 2, Kokubunji, Tokyo 185, Japan

Received February 4, 1991; in revised form June 3, 1991

The luminescence spectrum of $CsEu(MoO_4)_2$ is characterized by a single line at 614.5 nm, which has an intensity more than 10 times larger than any other visible line. This spectral feature can be ascribed to D_4 site symmetry, which is higher than the exact symmetry, D_2, derived from the space group. The apparent inconsistency results from the fact that Cs ions are located between layers consisting of (EuO_8) and (MoO_4) polyhedra with a long nearest-neighbor distance (0.475 nm) from Eu. A similar luminescence spectrum is observed also for $RbEu(MoO_4)_2$ except for line broadening due to random distribution of Rb and Eu ions. The luminescence of these compounds has high colorimetric purity resulting from the high probability of electric dipole transitions including the strong line at 614.5 nm.

1. Introduction

The luminescence spectrum of Eu^{3+} in condensed media is sensitive to the crystalline-field potential around Eu^{3+}. The $^5D_0 \rightarrow {}^7F_2$ emission, which is the most important component in red phosphors, gains its intensity when perturbation by odd-parity components of the crystalline-field potential breaks the otherwise forbidden selection rule (*1*). (As for the positions of the energy levels, see the diagram in Fig. 1.) The intensity ratio of the electric-dipole (e.g., $J = 0 \leftrightarrows 2$) to the magnetic-dipole transition (e.g., $J = 0 \leftrightarrows 1$) can be a good measure of the strength of the odd-parity component (*1*). In fact, commercial red phosphors, e.g., $Y_2O_2S:Eu^{3+}$ and $Y_2O_3:Eu^{3+}$, have high ratios of $J = 0 \rightarrow 2$ emission to $J = 0 \rightarrow 1$ emission (tentatively denoted as $I_{0\rightarrow2}/I_{0\rightarrow1}$ here) originating from the lack of inversion symmetry at the Eu^{3+} sites. The $I_{0\rightarrow2}/I_{0\rightarrow1}$ ratio is 12 for $Y_2O_2S:Eu^{3+}$ (4.3 mole%) and is even higher for $Y_2(WO_4)_3:Eu^{3+}$, though this material is not efficient enough for practical application (*2*).

This work reports another family of materials showing saturated red luminescence with a high $I_{0\rightarrow2}/I_{0\rightarrow1}$: alkali europium double molybdates, $AEu(MoO_4)_2$ where A = Cs, Rb, or K. For example, the ratio is 11 for A = Cs or Rb. Among the three, the double molybdates of Cs or Rb show an uncommon feature that a single emission line of the $^5D_0 \rightarrow {}^7F_2$ transition is by far stronger (10 times or more) than any other line in the visible region. As a result these materials show red luminescence of particularly high colorimet-

* To whom correspondence should be addressed.
† Present address: Takushoku University, Faculty of Engineering, 815-1, Tatemachi, Hachioji, Tokyo 193, Japan.

0022-4596/91 $3.00

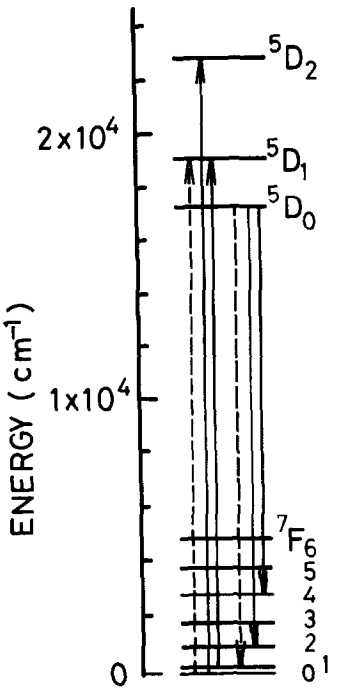

FIG. 1. The energy level diagram of Eu^{3+} (*14*). The degeneracy of each J state can be lifted by the crystalline-field potential. Solid lines indicate allowed electric dipole and broken lines allowed magnetic dipole transitions.

ric purity with the color coordinates x = 0.655 and y = 0.334. The aim of this work is to clarify the reason of this spectral feature, which is favorable to a red component of displays. Recently Van Vliet, Blasse, and Brixner presented the luminescence spectra of alkali europium double molybdates and tungstates as a means to classify the crystal structures of these compounds (*3*). This work focuses more on fine structures and discusses the site symmetry of Eu in $CsEu(MoO_4)_2$.

2. Experimental

(*a*) *Preparation of Samples*

Powder samples of the double molybdates were prepared by firing a stoichiometric mixture of Eu_2O_3, MoO_3, and alkali carbonates, all of four nine purity, in air for 2 to 4 days. The firing temperature was 625, 630, and 680°C for A = Cs, Rb, and K, respectively.

Crystal structures of the samples were analyzed by powder X-ray diffraction measurements. Observation by an optical microscope has shown that powder particles of $CsEu(MoO_4)_2$ and $RbEu(MoO_4)_2$ are flakes with irregular shapes.

Single crystals of $CsEu(MoO_4)_2$ with a typical dimension of 7 × 10 × 0.2 mm were obtained with spontaneous seeds. The stoichiometric melt was first kept at 1100°C for 2 hr and then cooled to 400°C with the average rate of 30°/hr. The crystals have a form of mica-like sheets with (100) cleavage planes. The growth method and observation on the crystals are essentially the same as reported by Van Uitert, Swanekamp, and Preziosi (*4*).

(*b*) *Optical Measurements*

Visible absorption spectra of single crystals were measured with a Hitachi Model 340 recording spectrophotometer. A polacoat sheet was used as a polarizer.

Luminescence spectra were measured with a Nikon P-250 monochromator which has a dispersion of about 6 nm/mm or with a Spex 1400 monochromator with about a 2 nm/mm dispersion. Data processing to calibrate spectral sensitivity of the measurement system, and to obtain relative luminance and color coordinates, was performed by using a Hewlett–Packard 9825A data acquisition system. The excitation source was a high pressure Hg lamp combined with a Toshiba UV-D1A glass filter and a cupric sulfate solution filter.

3. Results

(*a*) *Measurements of Powder X-Ray Diffraction*

Powder X-ray diffraction has shown that $CsEu(MoO_4)_2$ is an orthorhombic crystal

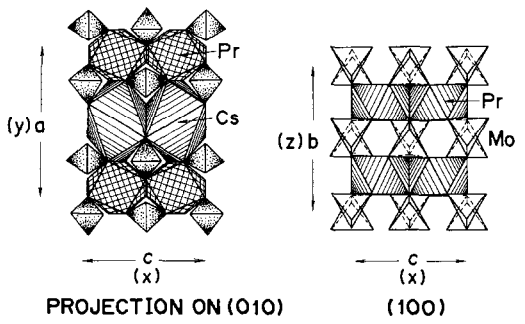

FIG. 2. Atomic arrangement in $CsPr(MoO_4)_2$ cited by Klevtsova, Vinokurov, and Klevtsov (*5*). The optical axis z is taken perpendicular to the rhombus of the twisted prism around Pr.

with the lattice parameters, $a_0 = 0.950$ nm, $b_0 = 0.508$ nm, and $c_0 = 0.807$ nm. These data agree well with the values reported by Klevtsova, Vinokurov, and Klevtsov (*5*). It was also found that $CsEu(MoO_4)_2$ shows a diffraction pattern similar to that of $CsPr(MoO_4)_2$ reported previously (*6*). According to Klevtsova, Vinokurov, and Klevtsov (*5*), the structure of $CsPr(MoO_4)_2$ belongs to the space group D_{2h}^3 with Pr and Cs ions coordinated with eight oxygen ions in a form of polyhedra which can be described as twisted prisms (see Fig. 2). The same species of polyhedra shares an edge and makes infinite ribbons in the (001) direction. In the (100) direction, the Pr and Cs polyhedra are joined alternately to form other infinite ribbons. The site symmetry of Pr is D_2, as can be observed in Fig. 2.

The cleavage plane of $CsEu(MoO_4)_2$ crystals was found to be the (100) plane. The b- and c-axes in the cleavage plane were determined by Laue and oscillation photographs.

As for $RbEu(MoO_4)_2$, it was reported in 1970 (*7*) that the low-temperature phase is isomorphous to orthorhombic $KY(MoO_4)_2$, which had been reported in 1968 (*8*) to belong to the space group $D_{2h}^{14} = P_{bcn}$. The site symmetry of Eu in this structure should be C_2. On the basis of these previous results, the lattice parameters of $RbEu(MoO_4)_2$ were calculated by using the X-ray diffraction data obtained in this work. The results thus obtained, $a_0 = 1.823$, $b_0 = 0.507$, and $c_0 = 0.795$ nm, reasonably agree with the previously reported values, $a_0 = 1.885$, $b_0 = 0.5132$, and $c_0 = 0.8123$ nm. It can be, therefore, concluded that $RbEu(MoO_4)_2$ prepared in this work has an orthorhombic structure isomorphous to $KY(MoO_4)_2$.

Powder X-ray diffraction data show that $KEu(MoO_4)_2$ is isomorphous with triclinic β-$KTb(MoO_4)_2$. The observed lattice parameters are $a_0 = 1.26$, $b_0 = 1.11$, $c_0 = 1.06$ nm, $\alpha = 90°30'$, $\beta = 89°$, and $\gamma = 114°24'$ in good agreement with the published data (*9*). The Eu site symmetry is reported to be C_1 (*10*).

(*b*) *Absorption and Luminescence Spectra of* $CsEu(MoO_4)_2$ *in the Visible Region*

In the following, the number of crystalline-field components is discussed for each J state based on the absorption and luminescence spectra.

Figures 3 and 4 show absorption spectra of $CsEu(MoO_4)_2$ single crystals measured at room temperature. The first $^7F_0 \rightarrow {}^5D_0$ line which should be observed at 582 nm (*3*) has a very small intensity and was not detected in this work.

The number of crystalline-field components of the $J = 1$ state is most probably two, because two narrow lines with different polarization are observed for $^7F_0 \rightarrow {}^5D_1$ absorption (Fig. 3). The absorption line peaked at 534.8 nm in the same figure is polarized, indicating the nature of an electric-dipole transition. Judged also from its wavelength region, this line can be assigned to the $^7F_1 \rightarrow {}^5D_1$ transition. It may involve two or more lines since its lineshape is asymmetrical. The weak and broad line that peaked at 540.5 nm is presumably vibronic, because the energy separation from the 534.8-nm line (197 cm^{-1}) is too large to be accounted for by the splitting of either the $^5D_1$ (7 cm^{-1}) or

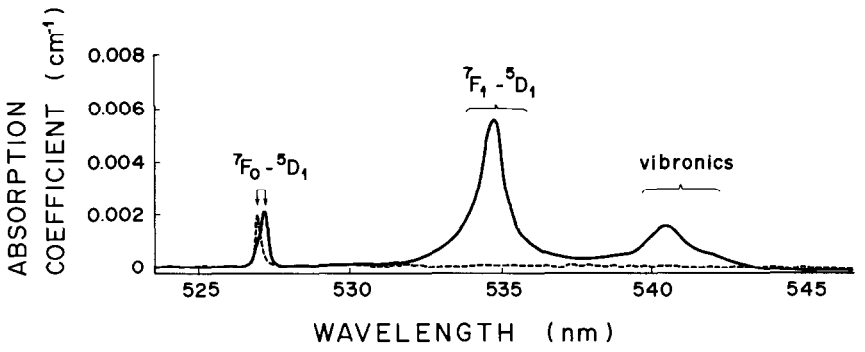

FIG. 3. The absorption spectra of $CsEu(MoO_4)_2$ at room temperature covering the $^7F_0 \rightarrow {}^5D_1$ and $^7F_1 \rightarrow {}^5D_1$ transitions. The spectra were measured with an electric vector parallel to the c (or x)-axis (solid line) or to the b (or z)-axis (broken line).

the $^7F_1$ state (31 cm^{-1}) obtained from the luminescence spectrum.

In the region of the $^7F_0 \rightarrow {}^5D_2$ transition (Fig. 4), a line at 465 nm has an intensity much larger than any other lines, as in the luminescence spectrum (Fig. 5). In addition to this, two weak lines can be observed in the polarization different from that of the strong line.

The spectrum of the $^7F_0 \rightarrow {}^5D_3$ transition indicates two lines at 416.8 and 417.2 nm, though they are not resolved well at room temperature (not shown).

Luminescence spectra were measured at 77 K. No difference was detected between the luminescence spectra of single crystals and those of powder samples. Figure 5 shows a luminescence spectrum in the

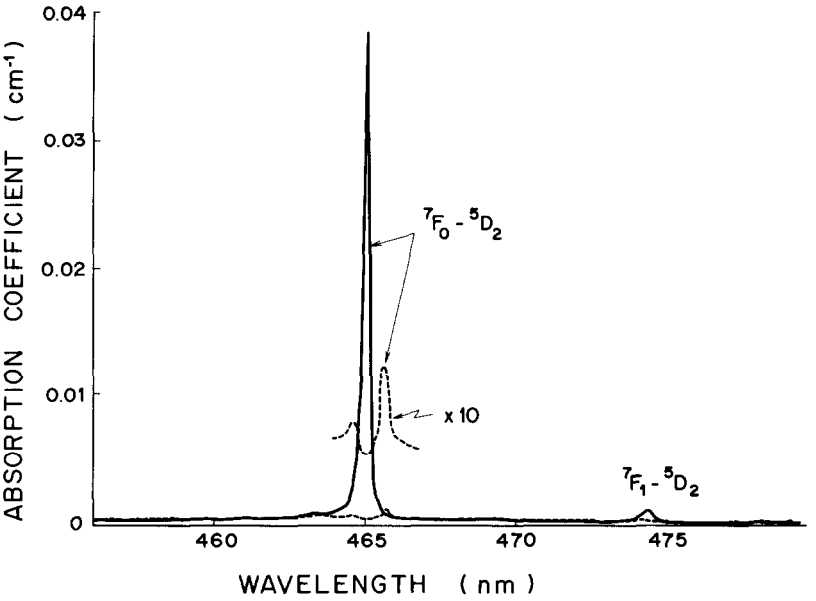

FIG. 4. The absorption spectra of $CsEu(MoO_4)_2$ at room temperature for the $^7F_0 \rightarrow {}^5D_2$ transition. The spectra were measured with an electric vector parallel to the c (or x)-axis (solid line) or to the b (or z)-axis (broken line).

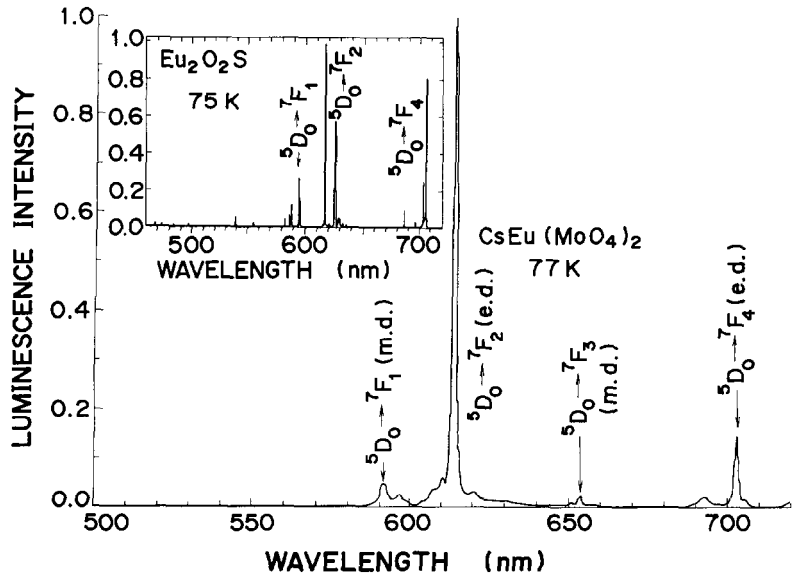

FIG. 5. The luminescence spectrum of $CsEu(MoO_4)_2$ powder in the whole visible region at 77 K. For comparison the luminescence spectrum of Eu_2O_2S at 75 K reported by Imanaga, Yokono, and Hoshina (*12*) is shown in the inset.

whole visible region to demonstrate that a single line dominates the spectrum. This spectral feature can be recognized more distinctively when compared with the spectrum of Eu_2O_2S given in the inset.

The $^5D_0 \rightarrow {}^7F_1$ spectrum is shown in Fig.

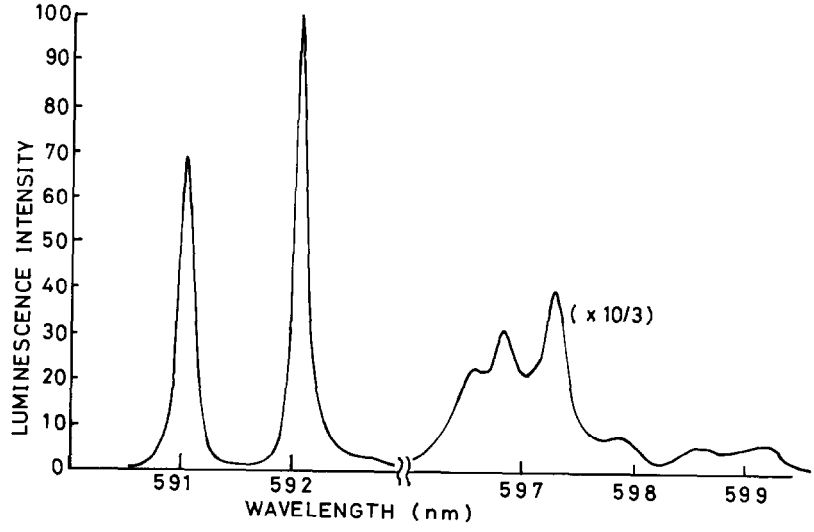

FIG. 6. The luminescence spectrum of $CsEu(MoO_4)_2$ powder for the $^5D_0 \rightarrow {}^7F_1$ transition at 77 K.

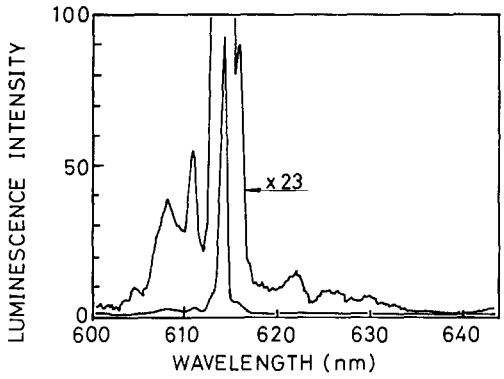

FIG. 7. The luminescence spectrum of $CsEu(MoO_4)_2$ powder for the $^5D_0 \rightarrow {}^7F_2$ transition at 77 K.

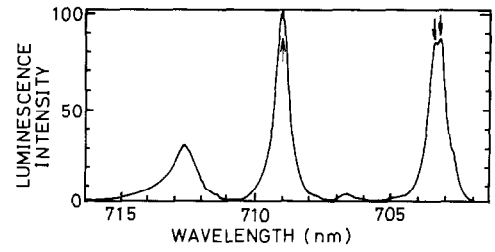

FIG. 8. The $^5D_0 \rightarrow {}^7F_4$ luminescence spectrum of $CsEu(MoO_4)_2$ powder at 77 K. The arrows indicate assumed electronic lines.

6. Two relatively strong lines are due to electronic transitions in agreement with the absorption spectrum, while weak lines at the longer wavelengths are considered to be vibronic lines.

In the region of the $^5D_0 \rightarrow {}^7F_2$ emission, three weak lines can be observed besides the dominant line at 614.5 nm (Fig. 7). Combined with the absorption spectra of the $^7F_0 \rightarrow {}^5D_2$ transition (Fig. 4), this result leads to a conclusion that the $J = 2$ state is split into three or four crystalline-field components but that only one transition is actually allowed.

For the $^5D_0 \rightarrow {}^7F_3$ emission only two lines are found at 651.3 and 654.2 nm, similar to the $^7F_0 \rightarrow {}^5D_3$ absorption spectrum (not shown).

The $^5D_0 \rightarrow {}^7F_4$ emission spectrum (Fig. 8) shows three fairly strong and narrow lines and two weak and broad lines. Judged from such lineshapes, the former three lines can be ascribed to electronic transitions, while the latter two are possibly of a vibronic nature.

(c) *Visible Luminescence Spectra of $RbEu(MoO_4)_2$ and $KEu(MoO_4)_2$*

The spectrum of $RbEu(MoO_4)_2$ is similar to that of $CsEu(MoO_4)_2$ (Fig. 9b). The Eu site symmetry is, therefore, the same as in $CsEu(MoO_4)_2$ as far as the nearest neighbor ions are concerned, but it is perturbed presumably by disordered distribution of Rb and Eu ions since the linewidths are broadened (*11*). If the $^5D_0 \rightarrow {}^7F_1$ transition is taken as an example, the width at half maximum of the narrower line is 4.1 cm^{-1} for CsEu

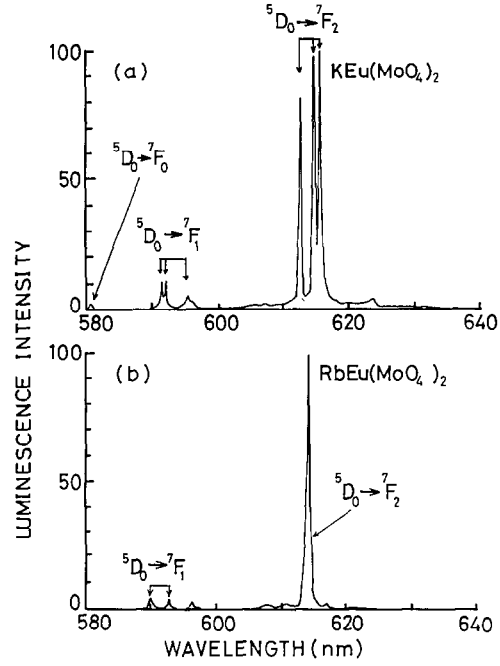

FIG. 9. The luminescence spectra of $KEu(MoO_4)_2$ (a) and of $RbEu(MoO_4)_2$ (b) both at 77 K.

$(MoO_4)_2$ and about 14 cm^{-1} for $RbEu(MoO_4)_2$ at 77 K.

The spectrum of $KEu(MoO_4)_2$ (Fig. 9a) shows that the Eu site symmetry is lower than the symmetry in $CsEu(MoO_4)_2$ or $RbEu(MoO_4)_2$; the $^5D_0 \rightarrow {}^7F_0$ transition is clearly observed, though the intensity is still small and three electronic lines appear with comparable intensities in the $^5D_0 \rightarrow {}^7F_2$ transition. The $^7F_1$ state is split into two or three components. And yet the site symmetry indicated by these features is higher than the reported site symmetry C_1, because under C_1 the number of emission lines should be 5 for $J = 0 \rightarrow 2$ transitions and a larger intensity is expected for $J = 0 \rightarrow 0$.

The distribution of K and Eu is also disordered, because the emission linewidths are broadened in this material, too (*11*). The width at half maximum of the $^5D_0 \rightarrow {}^7F_1$ line is as broad as that in $RbEu(MoO_4)_2$.

TABLE I

SELECTION RULES FOR TRANSITIONS FROM THE $J = 0$ STATE UNDER D_4 SYMMETRY

Terminal state	Type of crystal-field levels and allowed transitions	Number of observed electronic transitions
$J = 0$	A_1	0
$J = 1$	$A_2 (L_z)$	2
	$E (L_x, L_y)$	
$J = 2$	A_1, B_1, B_2	1 (strong) +
	$E (x,y)$	3–4 (very weak)
$J = 3$	B_1, B_2	2
	$A_2 (L_z)$	
	$2E (L_x, L_y)$	
$J = 4$	$2A_1, B_1, B_2$	3
	$A_2 (z)$	
	$2E (x,y)$	

Note. x, y, and z denote electric dipole transitions and L_x, L_y, and L_z magnetic dipole transitions (*13*).

4. Discussion

The observed numbers of crystalline-field components in $CsEu(MoO_4)_2$ cannot be accounted for by the D_2 symmetry expected from the space group; e.g., under D_2, three transitions are allowed to both $J = 1$ and 2 states from the $J = 0$ state. The result is that the observed numbers agree reasonably with the splitting under D_4 as shown in Table I. This means that the geometrical arrangement of neighboring ions around Eu can be regarded as D_4 symmetry, although the exact site symmetry is D_2. The local symmetry is approximately D_4 because the rhombic face of the oxygen polyhedra accommodating Eu (shown in Fig. 2) is actually very close to a square and the electrostatic effect of Cs ions upon Eu can be neglected. The latter condition seems plausible because Cs ions are located further away from Eu than O and Mo. (With the unit cell parameters of $CsEu(MoO_4)_2$ and atomic coordinates in $CsPr(MoO_4)_2$ (*5*), the nearest distance between Cs and Eu is estimated to be 0.475 nm, while it is 0.382 nm for Mo–Eu and 0.25 nm for O–Eu.) In this sense one can say that the layered structure is reflected in optical spectra of Eu^{3+}. The inconsistency of symmetry seen by $4f$ electrons with crystallographic site symmetry can take place because of the localization of $4f$ electrons.

This is also the case with $RbEu(MoO_4)_2$ and $KEu(MoO_4)_2$ as described in the last section. The inconsistency between crystallographic and spectroscopic site symmetry may be found also in other compounds containing loosely bound ions such as layered or clathrate compounds.

Acknowledgments

The authors are indebted to Dr. Jean-Pierre Jeser, presently a patent attorney at Burgundenstrasse 42, D-7100 Heilbronn, Germany for preparation of powder samples. They are also very grateful to Dr. Ojars J. Sovers at Jet Propulsion Laboratory, California Institute of Technology, for useful discussion on transition probabilities among crystal-field components of Eu^{3+}.

References

1. G. Blasse, A. Bril, and W. C. Nieuwpoort, *J. Phys. Chem. Solids* **27,** 1587 (1966).
2. T. Kano, K. Kinameri, and S. Seki, *J. Electrochem. Soc.* **129,** 2296 (1982).
3. J. P. M. van Vliet, G. Blasse, and L. H. Brixner, *J. Solid State Chem.* **76,** 167 (1988).
4. L. G. Van Uitert, F. W. Swanekamp, and P. Preziosi, *J. Appl. Phys.* **32,** 1176 (1961).
5. R. F. Klevtsova, V. A. Vinokurov, and P. V. Klevtsov, *Sov. Phys.-Crystallogr.* **17,** 240 (1972).
6. V. A. Vinokurov and P. V. Klevtsov, *Sov. Phys.-Crystallogr.* **17,** 102 (1971).
7. V. K. Rybakov, V. K. Truvov, and V. I. Spitsyin, *Dokl. Phys. Chem.* **192,** 393 (1970).
8. R. F. Klevtsova and S. V. Borisov, *Sov. Phys. Dokl.* **12,** 1095 (1968).
9. E. Ya. Pol'shikova and V. K. Trunov, *Russ. J. Inorg. Chem.* **15,** 587 (1970).
10. E. N. Ipatova, R. F. Klevtsova, and L. P. Solov'eva, *Sov. Phys.-Crystallogr.* **21,** 648 (1976).
11. H. Yamamoto, S. Seki, J-P. Jeser, and T. Ishiba, *J. Electrochem. Soc.* **127,** 694 (1980).
12. S. Imanaga, S. Yokono and T. Hoshina, *J. Luminescence* **16,** 77 (1978).
13. J. L. Prather, *NBS Monograph* **19,** 1 (1961).
14. G. H. Dieke and H. M. Crosswhite, *Appl. Opt.* **2,** 675 (1963).